Thermodynamic destabilization of azurin by four different tetramethylguanidinium amino acid ionic liquids

*Isabella DeStefano,[1]† Gabriella DeStefano,[1]† Nicholas J. Paradis,[1]† Roshani Patel,[1] Austin K. Clark,[1] Hunter Gogoj,[1] Gurvir Singh,[1] Keertana S. Jonnalagadda,[2,3] Aashka Y. Patel,[1] Chun Wu,[1,4] Gregory A. Caputo,[1,4] and Timothy D. Vaden[1,]**

† These authors contributed equally

1 Department of Chemistry and Biochemistry, Rowan University, Glassboro, NJ 08028, USA

2 Department of Biological Sciences, Rowan University, Glassboro, NJ 08028, USA

3 Bantivoglio Honors College, Rowan University, Glassboro, NJ 08028, USA

4 Department of Molecular and Cellular Biosciences, Rowan University, Glassboro, NJ 08028, USA

* To whom correspondence should be addressed:

Timothy D. Vaden
Department of Chemistry and Biochemistry
Science Hall, Office 301K
201 Mullica Hill Rd.
Rowan University
Glassboro NJ, 08028-1701
(856) 256 5457 (office)
vadent@rowan.edu

Keywords: ionic liquids; thermodynamic stability; molecular dynamics

Highlights

- The thermal stability of azurin was studied in the presence of 4 different ionic liquids
- The ionic liquids consisted of TMG as cation and different amino acid anions
- Experimental analysis revealed how ionic liquids affect unfolding enthalpies and entropies
- MD simulations qualitatively show how ionic liquids increase entropy of unfolded protein state

Abstract

The thermal unfolding of the copper redox protein azurin was studied in the presence of four different amino acid-based ionic liquids (ILs), all of which have tetramethylguanidium as cation. The anionic amino acid includes two with alcohol side chains, serine and threonine, and two with carboxylic acids, aspartate and glutamate. Control experiments showed that amino acids alone do not significantly change protein stability and pH changes anticipated by the amino acid nature have only minor effects on the protein. With the ILs, the protein is destabilized and the melting temperature is decreased. The two ILs with alcohol side chains strongly destabilize the protein while the two ILs with acid side chains have weaker effects. Unfolding enthalpy (ΔH°_{unf}) and entropy (ΔS°_{unf}) values, derived from fits of the unfolding data, show that some ILs increase ΔH°_{unf} while others do not significantly change this value. All ILs, however, increase ΔS°_{unf}. MD simulations of both the folded and unfolded protein conformations in the presence of the ILs provide insight into the different IL-protein interactions and how they affect the ΔH°_{unf} values. The simulations also confirm that the ILs increase the unfolded state entropies which can explain the increased ΔS°_{unf} values.

1. Introduction

Ionic liquids (ILs) have received significant interest as tunable biomaterials due to their abilities to alter protein structures, dynamics, and behaviors in aqueous solution [1-4]. ILs can stabilize or destabilize protein structures which makes them potential materials for industrial applications in which enzymes and other proteins need to function in non-physiological environments (high temperature, low pH, non-aqueous solvent, etc) [5-10]. Ideally, IL-based biomaterials can selectively stabilize desired proteins or protein structures while destabilizing or not affecting other proteins. For example, 1-ethyl-3-methylimidazolium chloride can assist in protein refolding for the β-sheet-rich recombinant plasminogen activator (rPA) but not for the α-helical protein lysozyme [11]. Further, cellulases can be designed via directed evolution to be more stable and more active in the presence of ILs in solution relative to the wild-type cellulases [4]. For example, the redox enzyme laccase from *Trametes versicolor* exhibits improved enzymatic activity at pH 5 compared to laccase alone at the same pH in the presence of ILs [12]. Different imidazolium-based ILs can increase enzyme activities (eg, for laccase) or inhibit enzymes (eg, for trypsin) [9].

Inherently, protein structure is directly linked to protein function, with many proteins losing enzymatic or binding capabilities as a result of only small disruptions in three-dimensional structure [13, 14]. As proteins fold co-translationally in the cell and often in the presence of chaperones and other specialized cellular structures, it has proven extremely difficult to recapitulate these conditions in an *in vitro* experiment. However, the denaturation of protein structures using changes in environmental temperature, pH, or through the addition of chemical denaturants (chaotropes) has yielded a tremendous amount of thermodynamic information on protein structural stability [15-20]. This approach has been extended to studies of proteins with ILs to gain a deeper understanding of the chemical functionalities within ILs and their impacts on protein stability. Not surprisingly, there have been a variety of studies reported which include protein stabilization and destabilization of a wide range of proteins in the presence of ILs [1, 9, 21-23]. Thus, it is critically important to develop a model to predict the effects of a given IL on the structure / function of a protein.

The promise of selective protein effects from ILs can be realized through their cation-anion "mix-and-match" tunability. IL properties, and IL effects on proteins, can in principle be tuned by changing the molecular cations and anions. ILs with cation and anion molecules that naturally have specific and selective biomolecular interactions with proteins can help increase the stabilization / destabilization selectivity. Ions in the Hofmeister series can be included as IL molecular anions due to their predictability in protein stabilization or destabilization [24-26]. The ability to tune IL formulations for specific biomolecular interactions can also be harnessed to reduce potential IL cytotoxic effects. In this context, amino acid-based ILs [27-31] have become an attractive option for biochemical and biotechnological applications, as these molecules are both "green" and highly biocompatible [27-29, 31-34].

Ohno et al. have developed amino acid-based ILs in which the anion is an amino acid [30, 31] that have been investigated for modulating protein folding [35]. The imidazolium-based cation used in these ILs may be bio-incompatible, but ILs using tetramethylguanidinium (TMG) as cations have been proposed for biotechnological applications [36]. The effects of TMG – amino acid (TMG-AA) ILs on the β-barrel protein mCherry have been studied using both experiments and simulations [22]. This study revealed that TMG cations have a destabilizing protein-IL interaction while the amino acid can either act to stabilize the protein (if anionic side chains are present), and hence offset the TMG destabilization, or not interact with the protein (if alkyl side chains are present), resulting in overall protein destabilization [22]. Thus, the competition between cation-protein and anion-protein interactions is highly sensitive to the selective amino acid – protein interactions. Further elucidating and quantifying these competitive interactions can help guide the understanding and development of TMG-AA ILs for protein applications.

Azurin is a small, mixed-structure copper-containing redox protein found in the periplasm of many Gram-negative bacteria as part of the cytochrome electron transport chain [37, 38]. Azurin, and related pseudoazurin proteins, also plays a central role in the denitrification process in many bacteria, which has made it a prime target for industrial applications [38-41]. Previously, infrared and vibrational circular dichroism spectroscopic studies of azurin in the presence of imidazolium chloride ILs showed how the more hydrophobic ILs increase unfolding rate constants and thermodynamically destabilize the protein structure

[42]. Importantly, thermal unfolding analysis showed that destabilization by ILs is, in the case of imidazolium chloride ILs, an entropic effect; ILs increase the value of the unfolding entropy which decreases the unfolding free energy [42]. Interpreting this conclusion can be greatly aided by molecular dynamics (MD) simulations. MD simulations have been invaluable for understanding the effects of ions and ionic liquids on protein structures and stabilities [2, 7, 43-47].

In this work, we use fluorescence spectroscopy and MD simulations to analyze and quantify the thermodynamic destabilization of azurin by four different TMG-AA ILs. The TMG-AA ILs, shown in Figure 1, include two species with alcohol side chains (tetramethylguanidine – serine, TMG-Ser, and tetramethylguanidine – threonine, TMG-Thr) and two species with carboxylic acid side chains (tetramethylguanidine – aspartate, TMG-Asp, and tetramethylguanidine – glutamate, TMG-Glu). Protein unfolding entropies and enthalpies are derived from thermal unfolding measurements for solutions of azurin with increasing IL concentrations. These measurements are compared to MD simulations that elucidate and characterize the amino acid interactions with the protein structure.

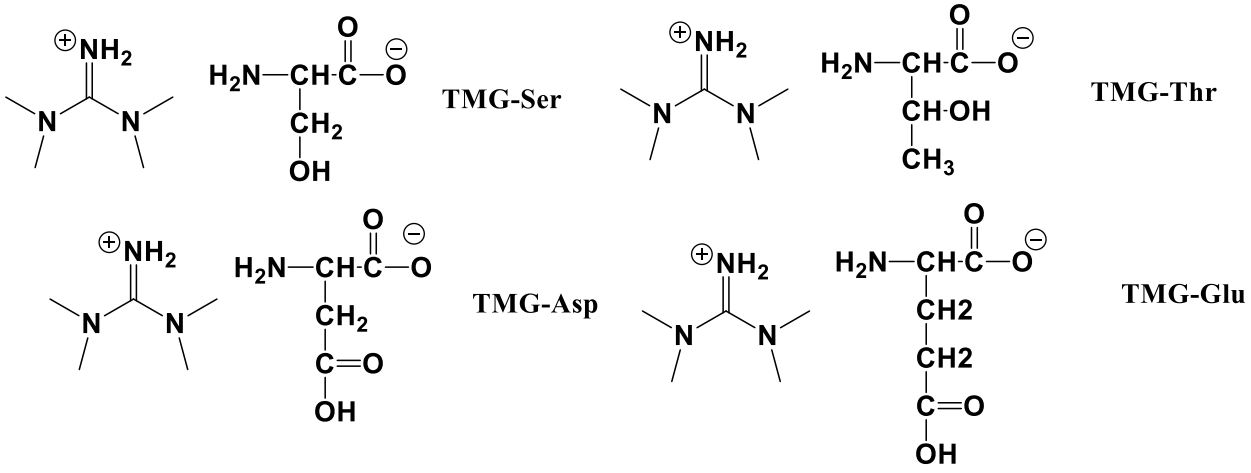

Figure 1. TMG-AA ILs used in this work. TMG-Ser and TMG-Thr have alcohol side chains while TMG-Asp and TMG-Glu have acid side chains.

2. Experimental Methods

2.1 Synthesis and purification of TMG-AA ILs

TMG-AA ILs were synthesized and purified as described previously [22]. Briefly, tetramethyl guanidine (Alfa Aesar, 99%), L-serine (Millipore Sigma), L-threonine (MP Biomedical), L-aspartic acid (Acros Organics), and L-glutamic acid (Fisher Scientific) were purchased and used without further purification. Under continuous nitrogen purge, tetramethylguanidine was added to a solution of the amino acid in distilled / deionized (DI) water in a 1:1 molar ratio and stirred for a few hours. The water was removed by vacuum evaporation at ~50 °C. 1.0 M stock solutions of the ILs in DI water were prepared directly from the pure ILs.

2.2 Expression and purification of azurin

The procedure for expressing and purifying azurin has been published [42]. To briefly summarize, plasmids expressing azurin from *P. aeruginosa* were purchased from Genscript (Piscataway, NJ) and used to transform chemically competent kanamycin-resistant *Escherichia coli* (*E. coli)*. Bacterial colonies grown on a kanamycin LB-agar plate were selected for growing in an LB broth supplemented with small amounts of magnesium sulfate and copper sulfate. Isopropyl β-D-1-thiogalactopyranoside (IPTG, Alfa Aesar) was added to the broth at 0.1 mM during growth to induce expression. Cells were centrifuged and then frozen until the protein purification procedure. For this procedure, cells were lysed by sonication in a buffer containing sucrose and ethylenediamine tetraacetic acid. After centrifugation the supernatant was subjected to acid precipitation in a pH 4.1 ammonium acetate buffer and then centrifuged. The azurin protein was purified from the supernatant by pH gradient chromatography using a CM sepharose column with ammonium acetate buffer. Copper chloride ($CuCl_2$) was added to the protein-containing fractions and then these fractions were further purified on a second CM sepharose column and eluted using a pH gradient procedure. The azurin-containing fractions were dialyzed overnight and the presence and purity of azurin was confirmed by gel electrophoresis.

2.3 Thermal unfolding of azurin using temperature-dependent fluorescence spectroscopy

IL stock solutions (1.0 M) were prepared from the pure ILs and DI water. Solutions of azurin (~0.1 mg/mL) with different concentrations and identities of ILs were prepared in DI water. Solution pH values were not controlled with buffers. To quantify how azurin is affected by pH, control experiments were performed in which azurin solutions (~0.1 mg/mL) were prepared with different buffers. The pH / buffers used were 20 mM acetate buffer (pH 4.0), 20 mM phosphate buffer (pH 6.0), 20 mM TRIS buffer (pH 8.0), and 20 mM ammonium hydroxide buffer (pH 10.0).

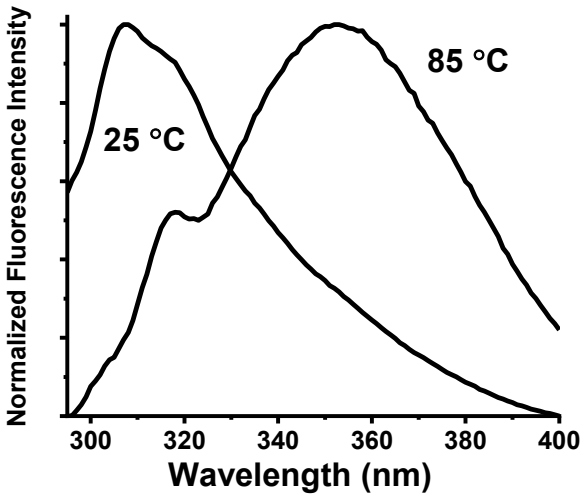

Figure 2. Normalized fluorescence spectrum of azurin at 25°C and 85°C.

Fluorescence spectra were recorded with a Horiba FluoroMax 4 spectrofluorometer. All samples were excited at 285 nm (exciting tryptophan residues) and emission spectra were recorded from 295 nm to 450 nm. The spectrometer is equipped with a Peltier-based temperature controller, and protein fluorescence spectra were recorded from 20 °C to 90 °C. Figure 2 shows the azurin fluorescence spectra at low temperature (where the protein is folded) and high temperature (where the protein is unfolded). The folded protein fluoresces at 308 nm while the unfolded protein fluoresces at 355 nm. At a given temperature, the normalized unfolded protein fraction (F_u) can be computed from the ratio of fluorescence intensities at 308 and 355 nm (I_{355}/I_{308}):

$$F_u = \frac{\left(I_{355}/I_{308}\right) - \left(I_{355}/I_{308}\right)_{folded}}{\left(I_{355}/I_{308}\right)_{unfolded} - \left(I_{355}/I_{308}\right)_{folded}} \quad (1)$$

Protein unfolding thermodynamic parameters ΔH°_{unf} and ΔS°_{unf} were derived from the experiments by fitting the following equation to the data (T is temperature in °C):

$$F_u = \frac{e^{\frac{-(\Delta H^{\circ}_{unf} - (T+273)\Delta S^{\circ}_{unf})}{R(T+273)}}}{\left(1+e^{\frac{-(\Delta H^{\circ}_{unf} - (T+273)\Delta S^{\circ}_{unf})}{R(T+273)}}\right)} \quad (2)$$

2.4 MD simulations

MD simulations were performed to analyze the stability of folded and unfolded azurin with and without the presence of TMG-AA ILs. A total of six systems were built: Folded azurin with water only, with TMG-Asp, and with TMG-Ser, and unfolded azurin with water only, with TMG-Asp, and with TMG-Ser (Table S1). Each system will be denoted by the azurin conformation (folded/unfolded) and associated solvent (water/TMG-Ser/TMG-Asp) starting here and throughout the manuscript. The folded systems were constructed using the high-resolution structure of azurin (PDB ID: 4MFH) from the RCSB Database (Figure 3A). The complete secondary structure is summarized in Figure S1 in the Supporting Materials. The unfolded systems were constructed from an unfolded structure (Figure 3B), which was obtained from a high temperature replica at 500 K of a Replica Exchange Molecular Dynamics (REMD) simulation started from the folded structure with temperature ranged from 300 K-500K (unpublished data). To reduce the computational cost, we focused only on two ILs, TMG-Ser and TMG-Asp, to investigate the differences between an alcohol side chain and an acid side chain. The azurin protein was prepared using the Protein Preparation Wizard of Maestro program [48]. Pre-processing and optimization of the pH 7 protonated state and geometry optimization used default parameters for restricted minimization. The ff14SB force field was used to represent the prepared azurin protein and the disulfide bonds within it. Ions characterizing the ILs

were prepared using AMBER16 software and the GAFF2 force field and manually added to the azurin system; the MOL2 files of TMG, Ser and Asp molecules are listed in the supporting document (Figures S2, S3, and S4 for TMG, Ser and Asp, respectively). Each IL system contained enough ions to constitute 0.1 M concentration. IL molecules were randomly placed around the protein and a relaxation protocol further randomized the IL molecular positions. Each system was built using the TIP3P water solvent model. Each system is contained in a solvent box of truncated octahedron using a 10 Å cut-off. Enough counter-ions were added to neutralize each system. The specifics of each system setup are tabulated in Table S1.

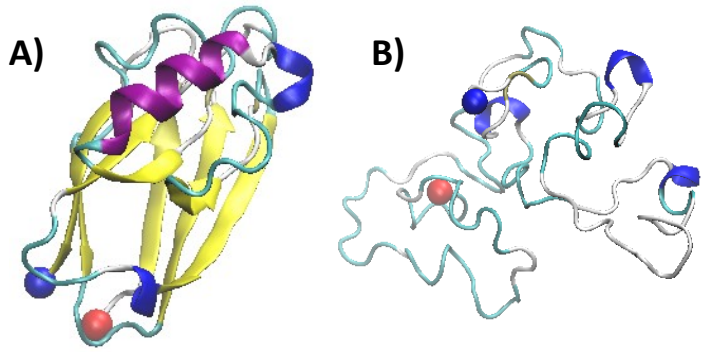

Figure 3: Reference structures. (A) Folded azurin; (B) unfolded azurin.

The simulation of each system was carried out using the AMBER 16 simulation package using standard simulation protocols. IL-containing systems (folded-TMG-Ser, folded-TMG-Asp, unfolded-TMG-Ser, and unfolded-TMG-Asp) had a 1,000 ps pre-run at 500 K to ensure that the position and orientation of TMG, Ser, and Asp molecules was randomized before a production run at 300 K. Azurin's position remained fixed during this pre-run. A production run at 300 K included a short 1.0 ns MD using the NPT ensemble mode (constant pressure and temperature) to equilibrate the system's density, followed by 999 ns dynamics in the equivalent NVT ensemble mode (constant volume and temperature). A validation plot is included in the supporting information (Figure S5) to demonstrate that the density of the bulk water of each system reaches ~1 g/ml after the 1.0 ns equilibration MD. All bonds interconnecting hydrogen atoms were treated with the SHAKE algorithm using a 2.0 fs time step in the simulations. Long-range electrostatic interactions were treated with the particle-mesh Ewald method [49] under periodic boundary conditions (charge grid spacing

of ~1.0 Å, the fourth order of the B-spline charge interpolation; and direct sum tolerance of 10^{-5}). Short-range non-bonded interactions were defined at 10 Å and long-range van der Waals interactions were based on a uniform density approximation. To reduce computation time and expense, non-bonded forces were calculated using a two-stage RESPA approach [50]. Short-range forces were updated every step and long-range forces were updated every two steps. The temperature was controlled using the Langevin thermostat with a coupling constant of 2.0 ps. The trajectories were saved every 50.0 ps for analysis purposes.

Root mean-squared deviation (RMSD) values were calculated for the azurin protein in each system. The RMSD of each system was calculated against their respective reference structures based on the azurin conformation. An additional RMSD plot was generated for the unfolded azurin systems with respect to the folded azurin crystal structure. To determine if refolding of native secondary structures occurred in the unfolded azurin trajectories, secondary structure plots were calculated for each amino acid residue for the folded and unfolded azurin systems using the Timeline plug-in tool from VMD [51]. The folded state plots were placed in the supporting document for comparison with the unfolded state plots to discover refolding in native protein regions. Root mean-squared fluctuation (RMSF) values were calculated for all individual residues in the azurin protein for the folded azurin systems to characterize the entropic change in the protein conformation in the folded state. A total of four atom contact plots were generated for folded-TMG-Ser, folded-TMG-Asp, unfolded-TMG-Ser, and unfolded-TMG-Asp, with a cut-off of 2.5 Å. These plots highlight (1) number of TMG-protein contacts, (2) number of ASP/SER-protein contacts, (3) protein polar side chain-IL interactions and (4) protein hydrophobic side chain-IL contacts.

3. Results

3.1 Thermal unfolding of azurin in the presence of ILs

The thermal unfolding results are summarized in Figure 4. For each IL, it can be seen that increasing IL concentration from 0.1 to 1.0 M decreases the melting temperature (T_m, the temperature at which the protein unfolds, or the temperature at which F_u is 0.5). Hence, all four ILs thermodynamically destabilize the azurin protein structure. The two TMG-AA ILs with carboxylic acid side-chains (TMG-Asp and TMG-Glu)

appear to have a somewhat weak destabilizing effect. Azurin in either DI water or pH 7 buffer unfolds at 82 °C. With TMG-Asp and TMG-Glu, T_m decrease down to ~70 °C with 0.1 M IL and to ~60 – 65 °C with 1.0 M IL. There also do not appear to be significant differences between Figure 4A and Figure 4B. This suggests that the shorter aspartic acid side chain and longer glutamic acid side chain have similar interactions with the protein. pH control experiments (Figure S6 in Supporting Information) show that pH values significantly lower (4) or higher (10) than pH 7 decrease T_m down to ~72 - 73 °C. The effects of TMG-Asp and TMG-Glu on azurin appear to be due to more than just pH-related effects as T_m values are below 70 °C at all IL concentrations.

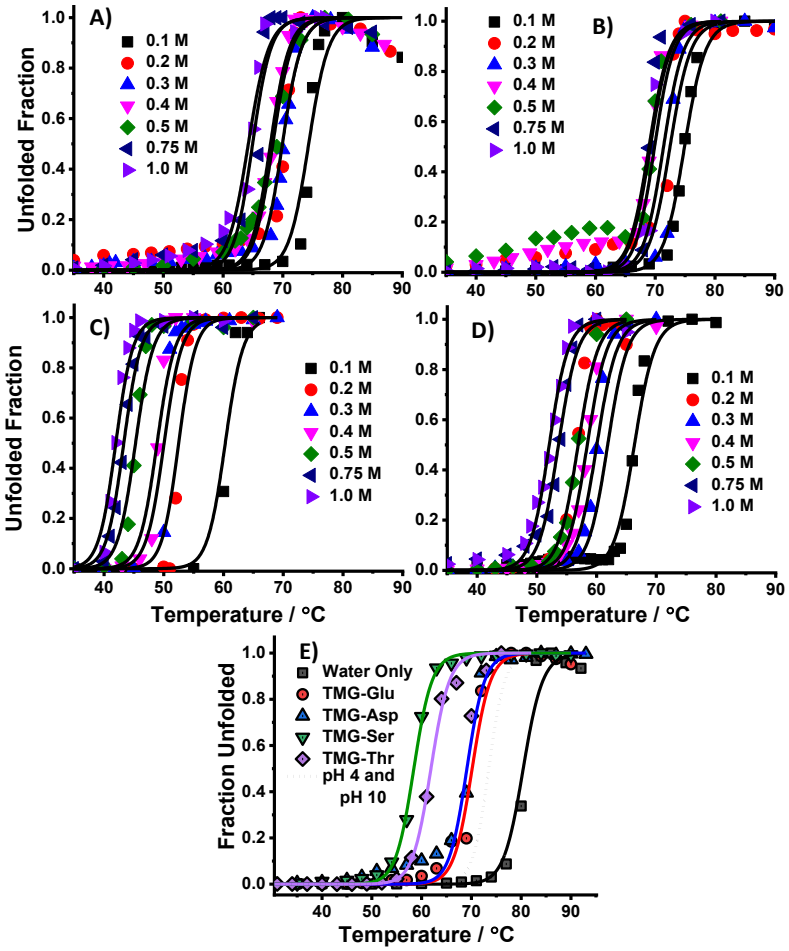

Figure 4. Unfolded fraction plotted against temperature for TMG-AA ILs with increasing concentration from 0.1M to 1.0 M. The data points are derived from the experimental fluorescence spectra and the solid lines are the best-fit functions from Equation (2). (A) TMG-Asp; (B) TMG-Glu; (C) TMG-Ser; (D) TMG-Thr; E) Summary of thermal unfolding results for azurin in the presence of 0.5 M ILs. The data for azurin

in water and different pH values are included for comparison. The data for pH 4 and 10 are identical (Figure S1) and are represented by a single curve.

The two TMG-AA ILs with alcohol side-chains, TMG-Ser (Figure 4C) and TMG-Thr (Figure 4D), appear to have a stronger destabilizing effect on azurin. T_m decreases from 82 °C (value for azurin in water) to ~40 – 60 °C for TMG-Ser and ~50 – 65 °C for TMG-Thr. As noted above, protein destabilization due to pH changes lowers T_m to ~72 – 73 °C, so the effects of TMG-Ser and TMG-Thr on azurin are clearly due to more than just pH changes. It is also clear from Figure 4 that TMG-Ser and TMG-Thr have different effects relative to each other. TMG-Ser has a stronger destabilizing effect on azurin relative to TMG-Thr. The difference between these two ILs is only an extra methyl chain on the Thr side-chain that slightly increases the hydrophobicity. This minor change in the IL molecular anion properties has a notable difference in how the IL affect the azurin protein structure.

The different destabilizing effects of the TMG-AA ILs on azurin are summarized in Figure 4E. The two ILs with acid side-chains, TMG-Asp and TMG-Glu, destabilize the azurin protein structure somewhat more than explainable by pH changes. These two ILs do not exhibit significant thermal unfolding differences between each other. The two ILs with alcohol side-chains, TMG-Ser and TMG-Thr, destabilize azurin significantly more than explainable by pH changes. TMG-Ser has a stronger effect than TMG-Thr. Thermal unfolding data for azurin with 0.5 M serine is shown in Figure S7. As serine alone does not destabilize azurin, the destabilization summarized in Figure 4 results from both the TMG and amino acid components in the IL and not just the amino acids. This is consistent with previous results for TMG-Ala in which alanine alone does not destabilize proteins [22].

The solid lines in Figure 4 shows the best-fit function using Equation (2). The unfolding thermodynamics values derived from these fits, ΔH°_{unf}, and ΔS°_{unf}, and T_m, are summarized in Figure 5. The data points at 0 M IL represent azurin in water and have been published previously [42]. The ΔH°_{unf} values (Figure 5A) show significant fluctuation that is likely due to statistical errors in the fitting parameters. However, some trends are clear. The two alcohol side-chain ILs, TMG-Ser and TMG-Thr, either slightly lower or leave unaffected the protein unfolding enthalpy while the two acid side-chain ILs, TMG-Asp and TMG-Glu, raise

the enthalpy. Hence from an energy perspective, the alcohol side-chain ILs have minimal effect while the acid side-chain ILs actually (energetically) stabilize azurin.

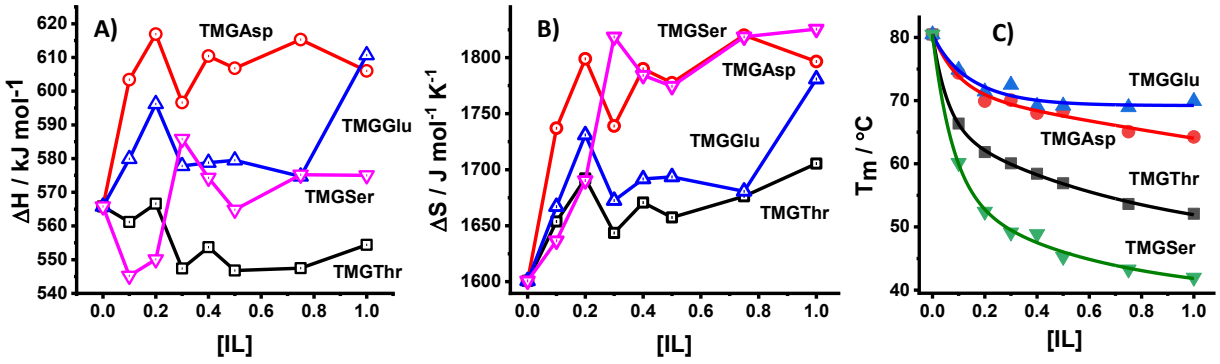

Figure 5. Summary of protein unfolding thermodynamic parameters azurin in the presence of TMG-AA ILs, all shown as functions of increasing IL concentrations.

The ΔS°_{unf} values, Figure 5B, also show clear trends. All four ILs increase the unfolding entropies. Increasing ΔS°_{unf} is a destabilizing effect as it results in a lower T_m value. Hence, the azurin destabilization by TMG-AA ILs appears to be an entropic effect rather than an energetic effect. Notably, while the TMG-Ser IL has the strongest entropic effect, TMG-Asp also has a strong effect on ΔS°_{unf} even though it has a weaker overall destabilizing effect (Figure 5C). Clearly TMG-Asp does not strongly destabilize azurin because it increases both ΔH°_{unf} and ΔS°_{unf} while TMG-Ser only increases ΔS°_{unf}. Also notable from Figure 5 is that while TMG-Ser and TMG-Thr have similar effects on T_m they have very different effects on ΔH°_{unf} and ΔS°_{unf}. TMG-Ser does not significantly change ΔH°_{unf} and increases ΔS°_{unf} while TMG-Thr slightly decreases ΔH°_{unf} and only moderately increases ΔS°_{unf}. Similarly, TMG-Asp and TMG-Glu have almost identical effects on T_m but quantitatively different effects on ΔH°_{unf} and ΔS°_{unf}. TMG-Asp produces large increases in both ΔH°_{unf} and ΔS°_{unf} while TMG-Glu produces only moderate changes in these values.

3.2 MD Simulations

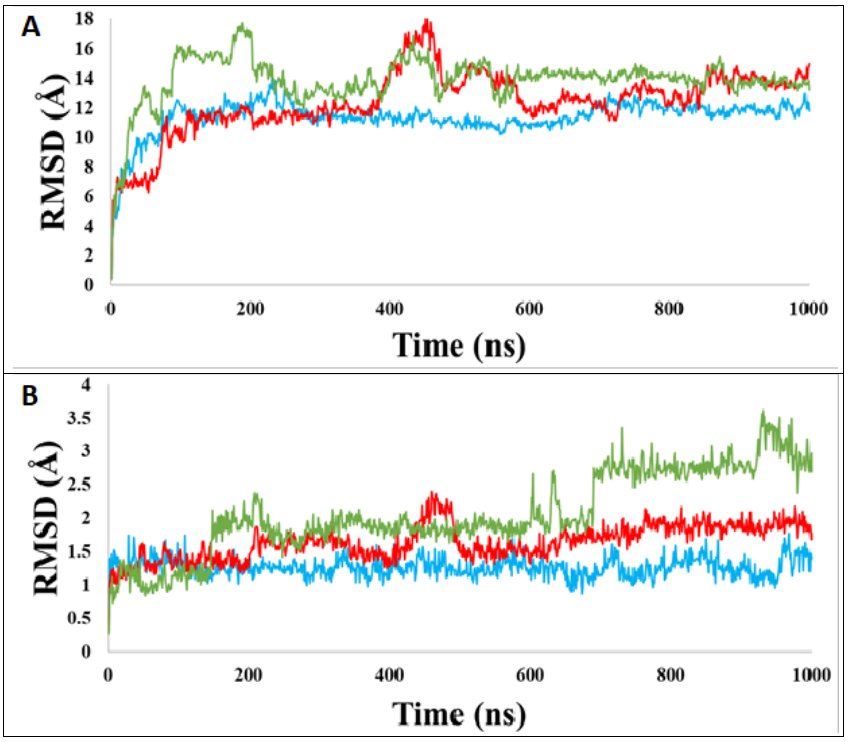

Figure 6. RMSD of azurin protein over 1000 ns in water (blue), TMG-Ser (green) and TMG-Asp (red). (**A**) Folded azurin. (**B**) Unfolded azurin.

RMSD trajectory plots over 1000 ns for folded and unfolded azurin are depicted for the protein backbone in Figure 6. For reference RMSD plots for unfolded azurin relative to the folded structure are shown in Figure S8. At room temperature folded azurin (Figure 6A) shows virtually no change in its conformation in the presence of water, TMG-Ser, or TMG-Asp compared to the folded reference structure (Figure 3A). This is illustrated by the average RMSD values for the last 300 ns for folded azurin (1.3 Å, 2.8 Å, and 1.9 Å for water, and TMG-Ser, and TMG-Asp, respectively). Protein instability is generally indicated by RMSD values well above 3.0 Å but such values are not seen in Figure 6B (RMSD increases with TMG-Ser and TMG-Asp are minor). Additionally, the azurin protein conformation was observed to be most stable with water and showed no unfolding events with TMG-Ser and TMG-Asp. This is consistent with the experimental results that show no unfolding at room temperature with or without ILs.

The RMSD plot for unfolded azurin shows a relaxation time at ~200 ns, reaching stable values of 11.8 Å, 14.0 Å, and 13.1 Å for unfolded-water, TMG-Ser, and TMG-Asp, respectively (Figure 6B).

Interestingly, the plot lines for each solvent between Figures 6A and 6B follow a similar trend. Water induces the least conformational change in the protein conformation but there are no significant changes with TMG-Ser or TMG-Asp.

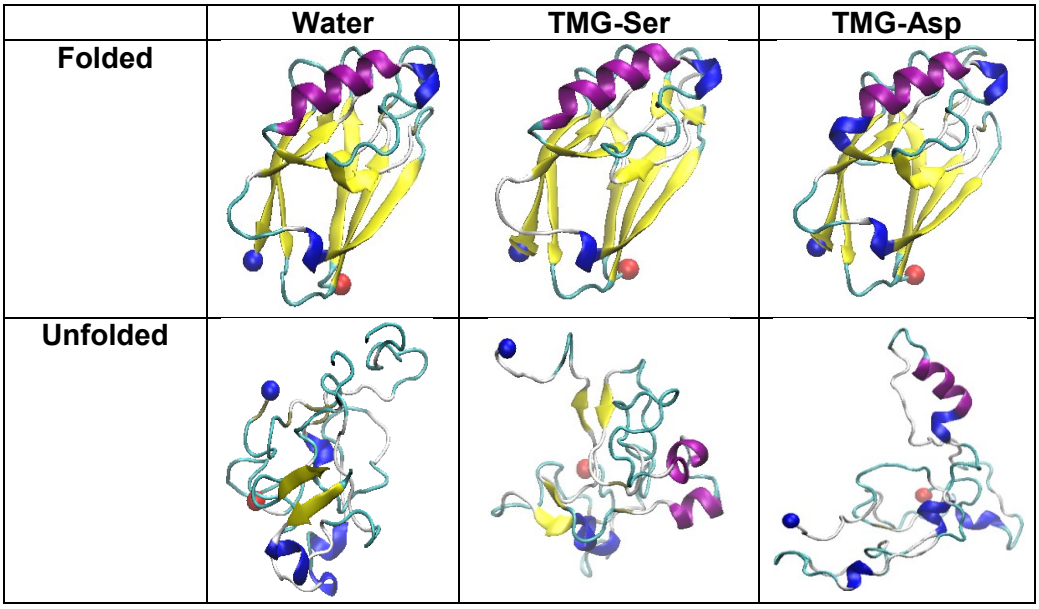

Figure 7. Last snapshot of folded and unfolded azurin protein structures in water, TMG-Ser, and TMG-Asp ILs. N- and C-termini are represented as red and blue spheres, respectively.

Interestingly, the MD simulations at 1 μs predict partial azurin structural refolding as shown in Figure 7. The degree of partial refolding varies between each IL compared to the unfolded reference structure (Figure 3B). With water, β-sheets and α-turns are formed, while with TMG-Ser, β-sheets and α-helices are formed, and with TMG-Asp, α-helices and additional α-turns are formed. To show a timeline of partial refolding, plot diagrams for each solvent are shown for both folded (Figure S9) and unfolded (Figure S10) azurin in the supporting materials. Simulations also predict partial refolding in both native and non-native protein regions of unfolded azurin (Figure S11). For instance, β-sheet strands formed in water (involving residues Lys85 - Asp93) and in TMG-Ser (Thr21), whereas α-helices formed in TMG-Asp (Met56 - Thr61). Simulations predict several instances of refolding in non-native regions of azurin. In water, azurin refolds to form transient α-helical (Phe97 - Lys101) and partial isolated β-bridges (Gly121 and Leu125). In TMG-

Ser, more significant α-helices form (Leu86 - Glu91 and Thr96 - Lys101). In TMG-Asp, α-helices refold to a lesser extent (Ile81 - Leu96). Under all solvent conditions, many instances of non-native 3-10 helical formation are also observed. This is not surprising, as 3-10 helices are proposed as intermediates in protein folding/unfolding processes. Nonetheless, the full refolding of azurin with a folding time ~7 ms [52] is still beyond the current computation power (1μs).

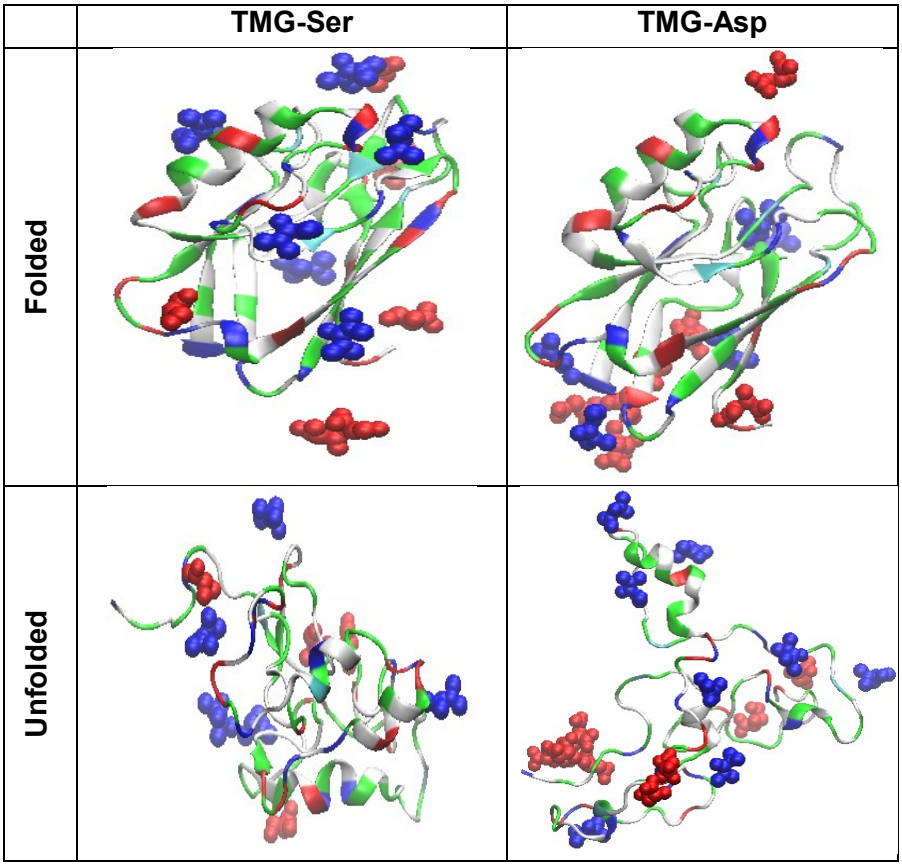

Figure 8. Distribution of TMG cations (blue) and Ser/Asp amino acid residues (red) in the last snapshot structures of folded (top row) and unfolded (bottom row) azurin protein. The protein is colored by residue type (i.e. acidic residues/red, basic residues/blue, hydrophobic residues/white and hydrophilic residues/green).

The interactions of TMG and Ser/Asp molecular ions with folded and unfolded azurin are depicted in Figure 8. Intermolecular contact plot diagrams for these systems are shown in Figure S12 and the average intermolecular contact values from the last 300 ns of these diagrams are summarized in Table 1. As

expected, TMG, Ser, and Asp molecules generally interact with anionic, polar, and cationic protein residues, respectively (Figure 8). Generally, IL-polar protein side chain interactions dominate (Figure S12). The folded azurin conformation only allows molecular sampling of its outer surface, providing some insight into the different observed molecular distributions in each solvent. In TMG-Ser, TMG and Ser molecular sampling is more evenly distributed across the protein surface (Figure 8). TMG is shown to assert protein contact dominance over Ser (23 and 11 protein contacts for TMG and Ser, respectively, Table 1). Not surprisingly, Ser engages more with polar versus hydrophobic protein side chains (30 and 7 for polar and hydrophobic side chains, respectively). For folded-TMG-Asp, TMG and Asp molecules cluster at the bottom portion of azurin (Figure 8). Here, protein contacts between TMG and Asp are nearly equivalent (30 and 33 protein contacts for TMG and Asp, respectively, Table 1). Unsurprisingly, Asp engages much more frequently with polar versus hydrophobic protein side chains (57 and 8 for polar and hydrophobic side chains, respectively).

In contrast to folded azurin, the hydrophobic interior of unfolded azurin is exposed to the surrounding solvent, subjecting the entire protein greater TMG, Asp, and Ser interactions, demonstrating greater molecular sampling of the protein. In unfolded-TMG-Ser, TMG seems to sample only one side of the protein, whereas Ser samples both sides (Figure 8). Contacts are summarized in Table 1. TMG once again dominates once more over Ser in protein contacts (19 and 11 protein contacts for TMG and Ser, respectively). Not surprisingly, Ser samples more polar side chains than hydrophobic side chains (24 and 7 for polar and hydrophobic side chains, respectively). In unfolded-TMG-Asp, the molecular distribution is more interesting. A distinct section of α-helices is positioned above the rest of the protein and demonstrates unique sampling. A trio of TMG cations is clustered around this isolated α-helical strand and throughout the rest of the protein, whereas Asp anions only sample the bottom portion (Figure 8). Here, Asp dominates significantly over TMG in protein contacts (23 and 62 protein contacts for TMG and Asp, respectively), exhibiting the highest protein contact count. Again, Asp interactions dominate with polar over hydrophobic protein side chains (76 and 11 for polar and hydrophobic side chains, respectively, Table 1). In both folded and unfolded azurin, Asp interacts with the protein more than Ser. This observation is strange, as we would

expect more significant sampling of the unfolded versus folded azurin conformation by both TMG-Ser and TMG-Asp, due to increased protein surface accessibility.

Table 1. Average contacts and standard deviation data for the folded and unfolded systems containing TMG-Ser and TMG-Asp.

System	Average Contacts (last 300 ns)			
	Protein-TMG	**Protein-Ser/Asp**	**Polar-IL**	**Hydrophobic-IL**
Folded-TMG-Ser	23±4	11±2	30±4	7±1
Unfolded-TMG-Ser	19±4	11±3	24±2	7±1
Folded-TMG-Asp	30±4	33±7	57±7	8±1
Unfolded-TMG-Asp	23±5	62±11	76±11	11±3

RMSF data are shown in Figure 9 for the folded and unfolded azurin systems and the average RMSF values for each system are summarized in Table 2. This data can be used to qualitatively infer the protein conformational entropy. Out of the three species, TMG-Ser induces the greatest entropic change to unfolded azurin (7.0 Å; change = + 5.6 Å) than water (4.9 Å; change = +3.8 Å) or TMG-Asp (6.1 Å; change = + 4.8 Å). However, the entropic effect of the protein contributed by TMG-Ser and TMG-Asp to azurin's folded conformation is minimal. In folded azurin (Figure 9A), residues 8-18 in TMG-Ser (a 6 Å peak) and residues 35-43 in the TMG-Asp system (a 4 Å peak) show noticeable fluctuations. Beyond residue 43, the protein maintains a 1 Å to 2 Å fluctuation range in all three systems. Additionally, RMSF values of the N- and C-termini vary slightly (~3.5 Å and ~2 Å, respectively) for each solvent. In the unfolded state (Figure 9B), almost no RMSF values superimpose in any of the systems, likely because the secondary structural features of each protein are different from varying solvent exposure. Only the first 24 residues are relatively stable among the three systems. Additionally, RMSF values of the N- and C-termini vary significantly (~3 Å and ~9 Å, respectively). Generally, unfolded azurin in water shows the greatest stability than in either TMG-

Asp or TMG-Ser, most noticeably around residues 70-82. Figure 9 appears to show that the unfolded protein state has higher disorder in the presence of the ILs, which is consistent with the experimental measurements.

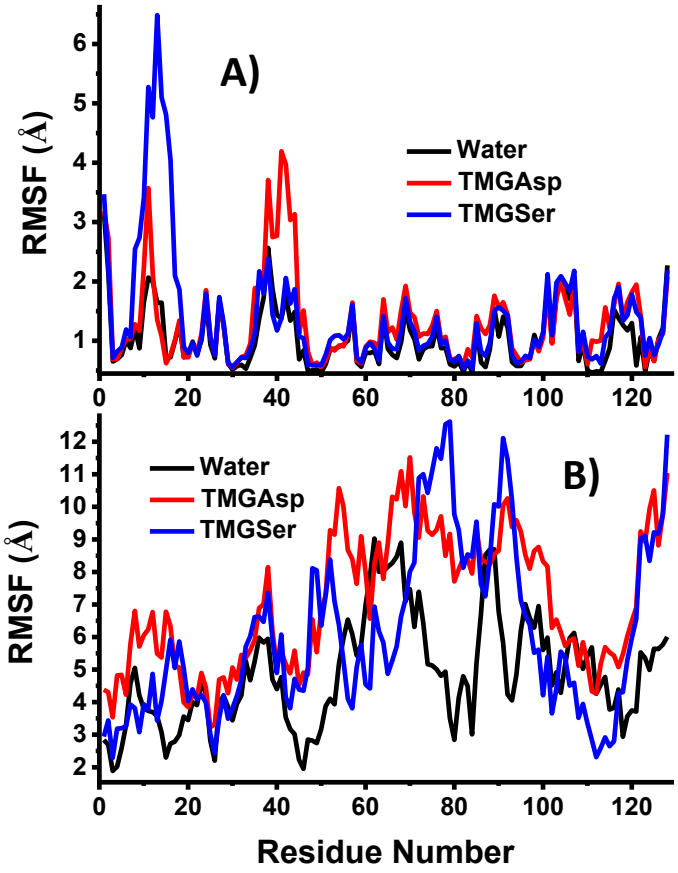

Figure 9. RMSF of folded azurin protein residues (1 to 128) in water (blue), TMG-Ser (green) and TMG-Asp (red). A) Folded protein; B) Unfolded protein.

Table 2. Average RMSF values of folded and unfolded azurin in water, TMG-Ser and TMG-Asp. The change in protein RMSF values is also shown.

System	Folded (Å)	Unfolded (Å)	Unfolded – Folded (Å)
Water	1.1 ± 0.5	4.9 ± 1.7	3.8
TMG-Ser	1.4 ± 0.7	7.0 ± 2.1	4.7
TMG-Asp	1.3 ± 1.0	6.1 ± 2.6	5.7

Experimental results (Figure 5) show a greater change in the entropy of unfolding (ΔS°_{unf}) in the TMG-Asp system (ΔS°_{unf} = 1760 $\frac{J}{mol \cdot K}$) than in the TMG-Ser system (ΔS°_{unf} = 1670 $\frac{J}{mol \cdot K}$). Both of these values are higher than the value of azurin in water (ΔS°_{unf} = 1588 $\frac{J}{mol \cdot K}$), which means ILs either decrease the folded state entropy or increase the unfolded state entropy. Table 2 shows RMSF values that can be compared with the experimental ΔS°_{unf} values to qualitatively characterize entropic effects of the protein. The simulations predict that the folded state entropy is not much affected by ILs but the unfolded state entropy increases with the ILs. ΔRMSF values (qualitative similar to ΔS°_{unf} values) in Table 2 are consistent with the experiments in suggesting an increased entropic impact of TMG-Ser and TMG-Asp (ΔRMSF = 4.7 Å and 5.7 Å for TMG-Ser and TMG-Asp, respectively) on azurin unfolding.

4. Discussion

The thermal unfolding experiments clearly show that TMG-AA ILs destabilize azurin in aqueous solution. The effect is not due simply to pH changes or amino acid interactions alone; destabilization is due to the IL molecular ions together. TMG-AA ILs in which the amino acid has an alcohol side chain (TMG-Ser and TMG-Thr) strongly destabilize azurin while those ILs with carboxylic acid side chains (TMG-Asp and TMG-Glu) have weaker effects. The unfolding thermodynamic parameters (ΔH°_{unf} and ΔS°_{unf}; derived from fitting Equation 2 to the data) reveal how overall thermal destabilization results from energetic and entropic changes to the protein in the presence of the ILs. TMG-Asp and TMG-Glu appear to increase both ΔH°_{unf} (leading to energetic stabilization) and ΔS°_{unf} (leading to entropic destabilization) resulting in modest protein destabilization overall. TMG-Ser and TMG-Thr also increase ΔS°_{unf} but do not affect ΔH°_{unf} much, resulting in overall stronger destabilization.

To understand how the ILs affect azurin and help interpret the thermodynamic results we performed MD simulations for both the folded and unfolded azurin structures in the presence of TMG-Ser and TMG-Asp. The room-temperature simulations show that the protein structure is stable with both ILs, which agrees with

the experiments; azurin does not unfold at room temperature in the presence of any of the ILs. The interactions between TMG, Ser, and Asp and the protein structure in both the folded and the unfolded state can provide insight into how the ILs affect ΔH°_{unf}. The current experimental results are consistent with literature reports that show increased ΔH°_{unf} values in the presence of ILs [42, 53, 54].

Together, Figures 8 and S12 elucidate how the IL molecular ions interact with the folded and unfolded protein states. First, it appears that Asp interacts with the folded protein structure more than Ser, and the Asp-protein interactions involve strong ionic forces rather than the weaker polar interactions favored by Ser. Hence, the simulations suggest that the folded state is energetically more stable with Asp than with Ser. Of course, the simulations show that the IL molecular ions interact with the unfolded state as well. However, Asp interacts more significantly with the unfolded state than with the folded state. Conversely, Ser appears to interact to about the same extent between the folded and unfolded states. Correlating the Asp-protein / Ser-protein interactions with conformational energy values is beyond the scope of our simulations. However, we can speculate that while the polar Ser - protein forces stabilize the folded state they probably have about the same effect on the unfolded state and the value of ΔH°_{unf} remains about the same as in water. In contrast, Asp clearly interacts with the folded and unfolded states differently which provides some simulation evidence that Asp will change ΔH°_{unf}. These simulation results then are consistent with the conclusion that due to the ionic Asp-protein interaction forces, TMG-Asp stabilizes the azurin folded state more than the unfolded state leading to an increased value of ΔH°_{unf} relative to water.

The TMG-AA IL effects on the ΔS°_{unf} values can be interpreted by the RMSF values in Table 2 and a visual inspection of Figure 7. Figure 7 shows that the folded azurin protein has about the same structure in the presence of water, TMG-Ser, and TMG-Asp, and Table 2 shows that RMSF values for the folded protein are about the same in these three cases. Hence, simulations suggest that the ILs do not significantly change the folded state protein entropy. The unfolded structures in Figure 7 are clearly different between water, TMG-Ser, and TMG-Asp. The protein appears to adopt a more disorganized conformation in the presence of the ILs and the structure is more disordered with TMG-Asp than with TMG-Ser. RMSF values for the

unfolded state in Table 2 are higher with the ILs than with water, and slightly higher with Ser than with Asp. These simulation results clearly support the conclusion that the ILs increase the entropy of the unfolded azurin structure leading to increased ΔS°_{unf} values. Experimentally, ΔS°_{unf} values are about the same between the two ILs but the simulation prediction that the unfolded entropy is higher with TMG-Ser than with TMG-Asp is certainly consistent with the lower T_m value for the former IL.

Together the experimental and MD simulation results show that the different effects between the TMG-AA ILs are due to the nature of the amino acid (from the IL) - protein interactions. The amino acids with alcohol side chains (Ser / Thr) prefer polar interactions that increase the entropy of the unfolded state, leading to an increased ΔS°_{unf} value, and stabilize both the folded and unfolded protein states, leading to negligible changes in ΔH°_{unf} values. The result is significantly decreased unfolding free energies and lower T_m values. The amino acid with the acid side chain (Asp / Glu) prefers ionic interactions that again increase the unfolded state entropy, and increase ΔS°_{unf}. The strong ionic interactions stabilize both the folded and unfolded protein states, but the experiments clearly show that the folded state must be stabilized more than the unfolded state. This increases ΔH°_{unf} and leads to unfolding free energies and T_m values that are not as low as with Ser / Thr.

While the effects of TMG-Thr and TMG-Glu were not studied with simulations (for time and cost reasons), the experiments show that they have generally similar effects as TMG-Ser and TMG-Asp, respectively. However, there are some important differences about which we can only speculate. The value of ΔS°_{unf} is significantly lower with TMG-Thr than with TMG-Ser, which is probably due to different strengths / natures of polar interactions due to the different side chain structures. Thr is slightly more hydrophobic than Ser due to the extra methyl group (Figure 1) which can affect the geometry of the IL-protein interaction. TMG-Glu has a weaker effect (relative to TMG-Asp) on both ΔH°_{unf} and ΔS°_{unf}, which is probably due to the overall weaker ionic forces related somehow to the longer side chain.

5. Conclusions

We investigated the thermal unfolding of azurin in the presence of four different TMG-AA ILs. The specific TMG-AA ILs include two species with alcohol side chains (TMG-Ser and TMG-Thr) and two species with acid side chains (TMG-Asp and TMG-Glu). The experimental results clearly show that the ILs destabilize the protein, with the two alcohol side-chain ILs having a stronger effect than the two acid side-chain ILs. Analyzing the thermal unfolding data provides ΔH°_{unf} and ΔS°_{unf} values. Clearly the ILs increase the entropic term, ΔS°_{unf}, but while the acid side-chain ILs increase the energetic term, ΔH°_{unf}, the alcohol side-chain ILs do not have much affect on ΔH°_{unf}.Thus, protein destabilization is due to an increase in unfolding entropy and the ILs that increase the unfolding energies have a weaker overall stabilization.

MD simulations on the folded and unfolded states of azurin in the presence of TMG-AA ILs elucidate how the ILs affect ΔH°_{unf} and ΔS°_{unf} values. Protein-IL interactions will change the energies of the folded / unfolded protein conformation. Simulations show that TMG interacts with the protein about the same in both states. Ser interacts with the protein via weaker polar interactions while Asp interacts via stronger ionic interactions, leading to the conclusion that Asp – azurin interactions energetically stabilizes the protein more than Ser – azurin interactions. Interestingly, while the Asp-protein contact doubles when the protein changes from the folded state to the unfolded state, Ser has similar contacts with the protein in both states. Additionally, we observed slightly higher helical content for the unfolded protein in TMG-Ser/Asp ILs than in the pure water, suggesting that these Ils appear to modulate the dielectric environment of the protein. We can arrive at a conclusion about how the ILs affect the protein energies by considering both the experimental and computational results. Ser probably stabilizes both the folded and unfolded protein state by about the same amount, while Asp more strongly stabilizes the folded protein state. Protein entropies can be qualitatively inferred from simulation fluctuation data, which show that the unfolded protein state fluctuations are greater with the ILs present. Hence, ILs increase the entropy of the unfolded state.

6. Acknowledgements

This work was supported by NSF grant DMR-1904797. CW thanks the computational support from NSF ACI-1429467, XSEDE MCB 170088 and from the Pittsburgh Supercomputing Center and D. E. Shaw Research under a grant MCB170090P.

References

[1] S. Jens, Aqueous ionic liquids and their effects on protein structures: an overview on recent theoretical and experimental results, J. Phys.: Condensed Matter 29(23) (2017) 233001.
[2] C. Schroder, Proteins in Ionic Liquids: Current Status of Experiments and Simulations, Topics in current chemistry (Journal) 375(2) (2017) 25.
[3] F. van Rantwijk, R.A. Sheldon, Biocatalysis in Ionic Liquids, Chem. Rev. 107 (2007) 2757-2785.
[4] A. Schindl, M.L. Hagen, S. Muzammal, H.A.D. Gunasekera, A.K. Croft, Proteins in Ionic Liquids: Reactions, Applications, and Futures, Frontiers in Chemistry 7(347) (2019).
[5] D. Constantinescu, C. Herrman, H. Weingartner, Patterns of protein unfolding and protein aggregation in ionic liquids, Phys. Chem. Chem. Phys. 12 (2010) 1756-1763.
[6] M. Naushad, Z.A. Alothman, A.B. Khan, M. Ali, Effect of ionic liquid on activity, stability, and structure of enzymes: A review, Int. J. Biol. Macromol. 51 (2012) 555–560.
[7] L. Bui-Le, C.J. Clarke, A. Bröhl, A.P.S. Brogan, J.A.J. Arpino, K.M. Polizzi, J.P. Hallett, Revealing the complexity of ionic liquid–protein interactions through a multi-technique investigation, Communications Chemistry 3(1) (2020) 55.
[8] A.J. Greer, J. Jaqcuemin, C. Hardacre, Industrial Applications of Ionic Liquids, Molecules 25 (2020) 5207.
[9] A.A.M. Elgharbawy, M. Moniruzzaman, M. Goto, Recent advances of enzymatic reactions in ionic liquids: Part II, Biochem. Eng. J. 154 (2020) 107426.
[10] S.P.M. Ventura, F.A. e Silva, M.V. Quental, D. Mondal, M.G. Freire, J.A.P. Coutinho, Ionic-Liquid-Mediated Extraction and Separation Processes for Bioactive Compounds: Past, Present, and Future Trends, Chem. Rev. 117(10) (2017) 6984-7052.
[11] M. Reslan, V. Kayser, Ionic liquids as biocompatible stabilizers of proteins, Biophys. Rev. 10(3) (2018) 781-793.
[12] A.P.M. Tavares, O. Rodriguez, E.A. Macedo, Ionic liquids as alternative co-solvents for laccase: Study of enzyme activity and stability, Biotech. and Bioeng. 101(1) (2008) 201-207.
[13] C.M. Dobson, Protein folding and misfolding, Nature 426(6968) (2003) 884-890.

[14] S.W. Englander, L. Mayne, The nature of protein folding pathways, Proc. Natl. Acad. Sci. 111(45) (2014) 15873-15880.
[15] D. Sanfelice, P.A. Temussi, Cold denaturation as a tool to measure protein stability, Biophysical Chemistry 208 (2016) 4-8.
[16] J.L. England, G. Haran, Role of solvation effects in protein denaturation: from thermodynamics to single molecules and back, Ann. Rev. Phys. Chem. 62 (2011) 257-77.
[17] R. Kazlauskas, Engineering more stable proteins, Chem. Soc. Rev. 47(24) (2018) 9026-9045.
[18] J.-H. Cho, D.P. Raleigh, Electrostatic interactions in the denatured state and in the transition state for protein folding: effects of denatured state interactions on the analysis of transition state structure, J. Mol. Biol. 359(5) (2006) 1437-1446.
[19] L. Smeller, Protein Denaturation on p-T Axes--Thermodynamics and Analysis, Sub-cellular biochemistry 72 (2015) 19-39.
[20] C.B. Anfinsen, The formation and stabilization of protein structure, Biochemical Journal 128(4) (1972) 737-749.
[21] A.Y. Patel, K.S. Jonnalagadda, N. Paradis, T.D. Vaden, C. Wu, G.A. Caputo, Effects of Ionic Liquids on Metalloproteins, Molecules 26(2) (2021).
[22] K.L. Borrell, C. Cancglin, B.L. Stinger, K.G. DeFrates, G.A. Caputo, C. Wu, T.D. Vaden, An Experimental and Molecular Dynamics Study of Red Fluorescent Protein mCherry in Novel Aqueous Amino Acid Ionic Liquids, J. Phys. Chem. B 121 (2017) 4823-4832.
[23] O.C. Fiebig, E. Mancini, G. Caputo, T.D. Vaden, Quantitative Evaluation of Myoglobin Unfolding in the Presence of Guanidinium Hydrochloride and Ionic Liquids in Solution, J. Phys. Chem. B 118 (2014) 406-412.
[24] Z. Yang, Hofmeister effects: an explanation for the impact of ionic liquids on biocatalysis, J. Biotechnology 144 (2009) 12-22.
[25] H. Zhao, Are ionic liquids kosmotropic or chaotropic? An evaluation of available thermodynamic parameters for quantifying the ion kosmotropicity of ionic liquids, J. Chem. Tech. & Biotech. 81(6) (2006) 877-891.
[26] R.L. Gardas, D.H. Dagade, J.A.P. Coutinho, K.J. Patil, Thermodynamic Studies of Ionic Interactions in Aqueous Solutions of Imidazolium-Based Ionic Liquids [Emim][Br] and [Bmim][Cl], J. Phys. Chem. B 112(11) (2008) 3380-3389.
[27] A.R. Shaikh, M. Ashraf, T. AlMayef, M. Chawla, A. Poater, L. Cavallo, Amino acid ionic liquids as potential candidates for CO2 capture: Combined density functional theory and molecular dynamics simulations, Chem. Phys. Lett. 745 (2020) 137239.
[28] L. Gontrani, Choline-amino acid ionic liquids: past and recent achievements about the structure and properties of these really “green” chemicals, Biophys. Rev. 10(3) (2018) 873-880.
[29] T. Tian, X. Hu, P. Guan, X. Ding, Research on solubility and bio-solubility of amino acids ionic liquids, J. Mol. Liquids 225 (2017) 224-230.
[30] K. Fukumoto, M. Yoshizawa, H. Ohno, Room Temperature Ionic Liquids from 20 Natural Amino Acids, J. Am. Chem. Soc. 127 (2005) 2398-2399.
[31] H. Ohno, K. Fukumoto, Amino Acid Ionic Liquids, Acc. Chem. Res. 40 (2007) 1122-1129.
[32] P. Ossowicz, J. Klebeko, B. Roman, E. Janus, Z. Rozwadowski, The Relationship between the Structure and Properties of Amino Acid Ionic Liquids, Molecules 24(18) (2019) 3252.
[33] C. Herrera, M. Atilhan, S. Aparicio, A theoretical study on mixtures of amino acid-based ionic liquids, Phys. Chem. Chem. Phys. 20(15) (2018) 10213-10223.
[34] M. Razmkhah, M.T. Hamed Mosavian, F. Moosavi, What is the effect of polar and nonpolar side chain group on bulk and electrical double layer properties of amino acid ionic liquids?, Electrochimica Acta 285 (2018) 393-404.
[35] K. Sankaranarayanan, G. Sathyaraj, B.U. Nair, A. Dhathathreyan, Reversible and Irreversible Conformational Transitions in Myoglobin: Role of Hydrated Amino Acid Ionic Liquid, J. Phys. Chem. B 116 (2012) 4175−4180.

[36] X. Ding, Y. Wang, Q. Zeng, J. Chen, Y. Huang, K. Xu, Design of functional guanidinium ionic liquid aqueous two-phase systems for the efficient purification of protein, Anal. Chem. Acta 815 (2014) 22-32.
[37] C. Arcangeli, A.R. Bizzarri, S. Cannistraro, Long-term molecular dynamics simulation of copper azurin: structure, dynamics and functionality, Biophysical Chemistry 78(3) (1999) 247-257.
[38] F. De Rienzo, R.R. Gabdoulline, M.C. Menziani, R.C. Wade, Blue copper proteins: A comparative analysis of their molecular interaction properties, Protein Science 9(8) (2000) 1439-1454.
[39] J. Leckner, P. Wittung, N. Bonander, B.G. Karlsson, B.G. Malmström, The effect of redox state on the folding free energy of azurin, J. Biol. Inorg. Chem. 2(3) (1997) 368-371.
[40] S. Horrell, D. Kekilli, R.W. Strange, M.A. Hough, Recent structural insights into the function of copper nitrite reductases, Metallomics : integrated biometal science 9(11) (2017) 1470-1482.
[41] E. Terasaka, K. Yamada, P.-H. Wang, K. Hosokawa, R. Yamagiwa, K. Matsumoto, S. Ishii, T. Mori, K. Yagi, H. Sawai, H. Arai, H. Sugimoto, Y. Sugita, Y. Shiro, T. Tosha, Dynamics of nitric oxide controlled by protein complex in bacterial system, Proc. Natl. Acad. Sci. 114(37) (2017) 9888.
[42] A. Acharyya, D. DiGiuseppi, B.L. Stinger, R. Schweitzer-Stenner, T.D. Vaden, Structural Destabilization of Azurin by Imidazolium Chloride Ionic Liquids in Aqueous Solution, J. Phys. Chem. B 123(32) (2019) 6933-6945.
[43] M. Chawla, I. Autiero, R. Oliva, L. Cavallo, Energetics and dynamics of the non-natural fluorescent 4AP:DAP base pair, Phys. Chem. Chem. Phys. 20(5) (2018) 3699-3709.
[44] B. Yoo, B. Jing, S.E. Jones, G.A. Lamberti, Y. Zhu, J.K. Shah, E.J. Maginn, Molecular mechanisms of ionic liquid cytotoxicity probed by an integrated experimental and computational approach, Scientific reports 6 (2016) 19889.
[45] M.P. Heitz, J.W. Rupp, Determining mushroom tyrosinase inhibition by imidazolium ionic liquids: A spectroscopic and molecular docking study, Int. J. Biol. Macromol. 107 (2018) 1971-1981.
[46] G.S. Lim, J. Zidar, D.W. Cheong, S. Jaenicke, M. Klahn, Impact of ionic liquids in aqueous solution on bacterial plasma membranes studied with molecular dynamics simulations, J. Phys. Chem. B 118(35) (2014) 10444-59.
[47] V.W. Jaeger, J. Pfaendtner, Destabilization of Human Serum Albumin by Ionic Liquids Studied Using Enhanced Molecular Dynamics Simulations, J. Phys. Chem. B (120) (2016) 12079-12087.
[48] G.M. Sastry, M. Adzhigirey, T. Day, R. Annabhimoju, W. Sherman, Protein and ligand preparation: Parameters, protocols, and influence on virtual screening enrichments, J. comput, Aid. Mol. Des. 27(3) (2013) 221-34.
[49] U. Essmann, L. Perera, M.L. Berkowitz, A smooth particle mesh Ewald method, J. Chem. Phys. 103 (1995) 8577-92.
[50] P. Procacci, B.J. Berne, MULTIPLE TIME-SCALE METHODS FOR CONSTANT-PRESSURE MOLECULAR-DYNAMICS SIMULATIONS OF MOLECULAR-SYSTEMS, Mol. Phys. 83(2) (1994) 255-272.
[51] W. Humphrey, A. Dalke, K. Schulten, VMD - Visual Molecular Dynamics, J. Molec. Graphics 14 (1996) 33-38.
[52] I. Pozdnyakova, P. Wittung-Stafshede, Copper Binding before Polypeptide Folding Speeds Up Formation of Active (Holo) Pseudomonas aeruginosa Azurin, Biochemistry 40(45) (2001) 13728-13733.
[53] P. Attri, P. Venkatesu, Exploring the thermal stability of α-chymotrypsin in protic ionic liquids, Process Biochemistry 48(3) (2013) 462-470.

[54] I. Jha, P. Attri, P. Venkatesu, Unexpected effects of the alteration of structure and stability of myoglobin and hemoglobin in ammonium-based ionic liquids, Phys. Chem. Chem. Phys. 16 (2014) 5514-5526.